Low-Temperature Rate Coefficients for Reactions of the Ethynyl Radical (C_2H) with C_3H_4 Isomers Methylacetylene and Allene

Ray J. Hoobler[†] and Stephen R. Leone*[,‡]

JILA, National Institute of Standards and Technology and University of Colorado, and Department of Chemistry and Biochemistry, University of Colorado, Boulder, Colorado 80309-0440

Received: October 5, 1998; In Final Form: January 6, 1999

Low-temperature rate coefficients for the reactions $C_2H + C_3H_4 \rightarrow$ products [C_3H_4 = methylacetylene (propyne) CH_3CCH and allene (propadiene) CH_2CCH_2] are measured over the temperature range of 155−298 K. Absolute rate constants are determined using laser photolysis and transient infrared absorption spectroscopy. Both reactions are fast, approaching the kinetic limit and have either no temperature dependence or a slight negative temperature dependence. Over the experimental temperature range, the rate constants are fit to the following Arrhenius expressions: $k_{CH_3CCH} = (1.6 \pm 0.4) \times 10^{-10} \exp[(71 \pm 50)/T]$ cm^3 molecule^{-1} s^{-1} and $k_{CH_2CCH_2} = (1.3 \pm 0.6) \times 10^{-10} \exp[(103 \pm 136)/T]$ cm^3 molecule^{-1} s^{-1}. The corresponding rate constants at 298 K are $k_{CH_3CCH} = (1.9 \pm 0.3) \times 10^{-10}$ cm^3 molecule^{-1} s^{-1} and $k_{CH_2CCH_2} = (1.7 \pm 0.3) \times 10^{-10}$ cm^3 molecule^{-1} s^{-1}. These measurements provide new reaction rate coefficients for the ethynyl radical, C_2H, with C_3H_4 unsaturated hydrocarbons. These are necessary to extend current photochemical models of Jupiter, Saturn, and its satellite Titan.

Introduction

The study of neutral radical−molecule reactions is of interest in several diverse fields including combustion science, terrestrial atmospheric chemistry, and planetary atmospheric chemistry. With the launch of the Cassini/Huygens mission to Saturn and its largest satellite Titan in the fall of 1997 and the ongoing Galileo mission to Jupiter, there is continuing interest in understanding the photochemical processes that take place in these planetary atmospheres.[1] Titan is of particular interest due to its dense N_2-CH_4 atmosphere, which may have similarities to that of the prebiotic atmosphere of Earth.[2]

Over the past several years, there have been two new photochemical models of Titan's atmosphere.[3,4] These models are in addition to the first post-Voyager models of Titan's atmosphere by Yung *et al*.[5,6] In addition, a recent photochemical model of Jupiter's upper atmosphere has also been put forth.[7] An important requirement for accurate photochemical models is a complete database of rate coefficients that cover an appropriate temperature range. Unfortunately, in many cases, low-temperature rate coefficients are not available and values must be extrapolated from high-temperature results, theory, or analogy. As modelers strive to be more complete in detailing photochemical processes of these complex systems, the need for accurate laboratory data continues to grow.

The ethynyl radical is an important chemical species in planetary atmospheres, especially Titan's. Models cite hydrogen abstraction processes as key steps in the propagation of free radicals that ultimately produce larger organic molecules by radical−radical association reactions. Direct photolysis and photolysis of species such as the ethynyl radical contribute to these processes, and both saturated and unsaturated hydrocarbons participate in radical−radical association reactions. In addition, ethynyl and other radicals can also react with unsaturated hydrocarbons via addition/elimination mechanisms. These reactions also lead to the formation of larger organic molecules and polymers.

In previous measurements, the low-temperature rate coefficients for C_2H with C_2H_2,[8] CH_4,[9] C_2H_4, C_2H_6, H_2,[10] C_3H_8, C_4H_{10}, C_5H_{12},[11] HCN, CH_3CN,[12] and O_2[13] have been studied. Here, absolute rate coefficients for the reactions of C_2H with the C_3H_4 unsaturated hydrocarbons methylacetylene (propyne) and allene (propadiene) are measured over the temperature range 150−298 K.

$$C_2H + CH_3CCH \rightarrow \text{products} \quad (1)$$

$$C_2H + CH_2CCH_2 \rightarrow \text{products} \quad (2)$$

Limited experimental data to define the products of reaction 1 are available,[14] and rate coefficients for reactions 1 and 2 have only been estimated from a shock-tube study of allene pyrolysis (1300 K < T < 2000 K).[15] Hydrogen abstraction, addition, and addition/elimination reactions are thermodynamically possible.

$$\begin{aligned} \dot{C}_2H + CH_3CCH &\rightarrow C_2H_2 + \dot{C}H_2CCH \\ &\rightarrow C_2H_2 + CH_3C\dot{C} \\ &\rightarrow C_4H_2 + \dot{C}H_3 \\ &\rightarrow C_5H_4 + \dot{H} \\ &\rightarrow C_5H_5^{\bullet} \end{aligned} \quad (3)$$

* Corresponding author.
[†] Permanent address: Department of Chemistry, University of South Alabama, Mobile, AL 36688.
[‡] Staff Member, Quantum Physics Division, National Institute of Standards and Technology.

10.1021/jp9839596 CCC: $18.00
Published on Web 02/20/1999

$$\dot{C}_2H + CH_2CCH_2 \rightarrow C_2H_2 + CH_2C\dot{C}H$$
$$\rightarrow C_5H_4 + \dot{H}$$
$$\rightarrow C_5H_5^{\bullet} \quad (4)$$

Note that the $\dot{C}H_2CCH$ and $CH_2C\dot{C}H$ species are resonance structures, shown this way to indicate the location of the removed hydrogen. The structures of the addition species are not considered here. All of the above reactions are highly exothermic, -200 kJ mol^{-1} < ΔH_{rxn} < -80 kJ mol^{-1}, with the exception of $C_2H + CH_3CCH \rightarrow C_2H_2 + CH_3C\dot{C}$, which is thermoneutral. Values for ΔH_{rxn} are obtained from reported heats of formation or values based on group additivities.[16,17] In related studies, the addition of Cl to C_3H_4 species has been described in detail recently.[18]

Results presented here are the first reported absolute rate coefficients for the reactions of the ethynyl radical, C_2H, with the C_3H_4 isomers methylacetylene (propyne) CH_3CCH and allene (propadiene) CH_2CCH_2. While all of these chemical species are included in recent photochemical models of Titan and Jupiter, which have made strong progress incorporating the chemistry of three and four carbon hydrocarbons, the reactions of the ethynyl radical with methylacetylene and allene have not been included. Results show that both of these reactions occur rapidly. The reactions studied here may represent important paths in the removal of the ethynyl radical and may be a source of larger unsaturated hydrocarbons in these planetary atmospheres.

Experiment

Details of the experiment have been described in several previous publications and only a brief summary will be presented here.[8,9] Experiments are carried out in a variable-temperature transverse flow cell. The 2.5 cm diameter 100 cm long flow cell is made of quartz and is surrounded by an insulated outer jacket. Gases are introduced and removed from the cell by a series of transverse inlets and pump-outs. This arrangement allows for the rapid removal of the photolysis products from the flow cell. Experiments are carried out at pressures between 1.3 and 12 kPa (10−90 Torr) with typical pressures in the flow cell being 3.7−4.1 kPa (28−31 Torr). Partial pressures for each gas are calculated from the measured flow rates using calibrated mass flow meters. Number densities for C_2H_2 and C_3H_4 are $(2-6) \times 10^{14}$ and $(2-16) \times 10^{14}$ molecules cm^{-3}, respectively, with the balance being helium. On the basis of available cross sections for allene and methylacetylene, loss due to their photolysis is estimated to be no greater than 2% and 3%, respectively.[19] Reactant concentrations are not corrected for this loss process. All gases flow through a mixing cell before entering the flow cell. He (99.99% pure), CH_3CCH (99%), and CH_2CCH_2 (97%) were obtained from commercial sources and used as received. The trace acetone in the C_2H_2 (99.6% pure) is removed by an activated charcoal filter. A temperature range of 150−298 K is obtained by circulating cold isopentane or pentane through the outer jacket. Cooling is obtained by flowing the (iso)pentane through a copper coil submerged in an ethanol−liquid nitrogen slush. Temperatures are measured at three positions along the length of the cell to ensure that temperature gradients are minimized.

Ethynyl radicals are produced by laser photolysis of acetylene (C_2H_2) using the 193 nm output of an ArF excimer laser. The excimer laser is typically run at 10−15 Hz and the pulse energy entering the flow cell is ≈40 mJ. Using a reported cross section of 1.35×10^{-19} cm^{-2} and a quantum yield of 0.26, we estimate an upper limit for $[C_2H]$ to be 4×10^{11} molecules cm^{-3}.[20] The transient ethynyl concentration is probed by a single-mode F-center laser operating at 3593.68 cm^{-1}, which corresponds to the $Q_{11}(9)$ line of the $A^2\Pi-X^2\Sigma^+$ (000) transition.[21] The longitudinal mode structure of the F-center laser is monitored with a scanning Fabry-Perot spectrum analyzer. The wavelength is determined by a traveling wave meter.[22] The photolysis and probe lasers are overlapped throughout the full length of the flow cell, and the infrared probe beam is multipassed three times to increase the absorption path length. The probe beam is directed onto a 77 K 50 MHz Ge:Au infrared detector that has a sensitive area of 20 mm^2. The transient absorption signals are amplified and then co-added using a digital oscilloscope. Typically, 1500−5000 traces are averaged before the data is transferred to a personal computer for analysis.

Results

Rate coefficients are measured under pseudo-first-order conditions where $[C_3H_4] \gg [C_2H]$, as noted above. The rate of change for $[C_2H]$ is given by

$$d[C_2H]/dt = -[C_2H](k_{C_3H_4}[C_3H_4] + k_{C_2H_2}[C_2H_2]) \quad (5)$$

After integration

$$[C_2H] = [C_2H]_0 \exp[-k_{obs}(t)] \quad (6)$$

where

$$k_{obs} = k_{C_3H_4}[C_3H_4] + k_{C_2H_2}[C_2H_2] \quad (7)$$

Two methods are used to obtain the rate constant, $k_{C_3H_4}$. The rate coefficient $k_{C_2H_2}$ was previously determined in our laboratory over the temperature range 150−360 K.[8,9] Since $[C_2H_2]$ is also known, the observed decay can be corrected for contributions due to reaction of C_2H with the precursor C_2H_2.

$$k_{obs} - k_{C_2H_2}[C_2H_2] = k_{C_3H_4}[C_3H_4] = k'_{C_3H_4} = k' \quad (8)$$

The contribution of $k_{C_2H_2}[C_2H_2]$ to k_{obs} is between 10% and 60% and <40% for most measurements. The observed decay rates, k_{obs}, are obtained by fitting the transient signal to the following equation:

$$y = A \exp[-k_{obs}(t)] + \text{const} \quad (9)$$

where the constant is just a dc offset in the signal. A typical transient signal is shown in Figure 1; 25−35 measurements are made at each temperature. After subtracting contributions from reactions of C_2H with the C_2H_2 precursor, the values of $k'_{C_3H_4}$ are plotted vs $[C_3H_4]$ with the resulting slope being equal to $k_{C_3H_4}$.

An equivalent method is to express concentrations as mole fractions

$$k_{obs} = [k_{C_3H_4}X_{C_3H_4} + k_{C_2H_2}X_{C_2H_2}]([C_3H_4] + [C_2H_2]) \quad (10)$$

with $X_{C_3H_4}$ and $X_{C_2H_2}$ being the mole fraction of each gas. By definition, $X_{C_3H_4} + X_{C_2H_2} = 1$. A plot of the quantity k^* (eq 11) vs the mole fraction $X_{C_3H_4}$ becomes

$$k^* = k_{obs}/([C_3H_4] + [C_2H_2]) = k_{C_3H_4}X_{C_3H_4} + k_{C_2H_2}(1 - X_{C_3H_4}) \quad (11)$$

The value of $k_{C_3H_4}$ is obtained from a linear least-squares fit of

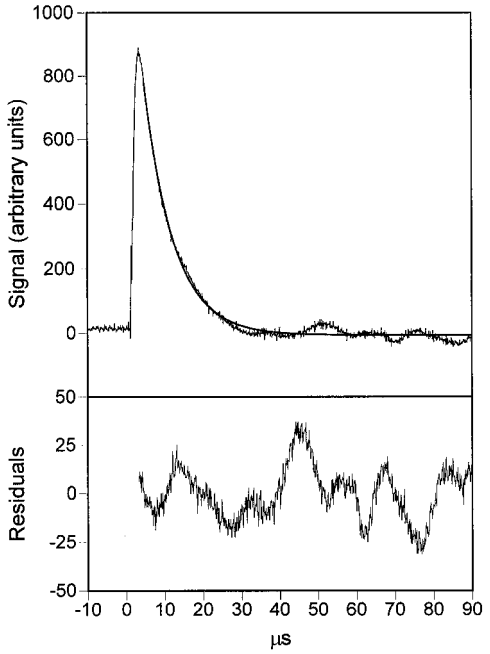

Figure 1. (Upper trace) Typical C_2H transient absorption signal at 297 K. Total pressure 12.3 kPa, $[C_2H_2] = 2.5 \times 10^{14}$ molecules cm^{-3}, $[CH_2CCH_2] = 6.1 \times 10^{14}$ molecules cm^{-3}, $k_{obs} = 0.144\ \mu s^{-1}$. (Lower trace) Residuals to fitted experimental decay.

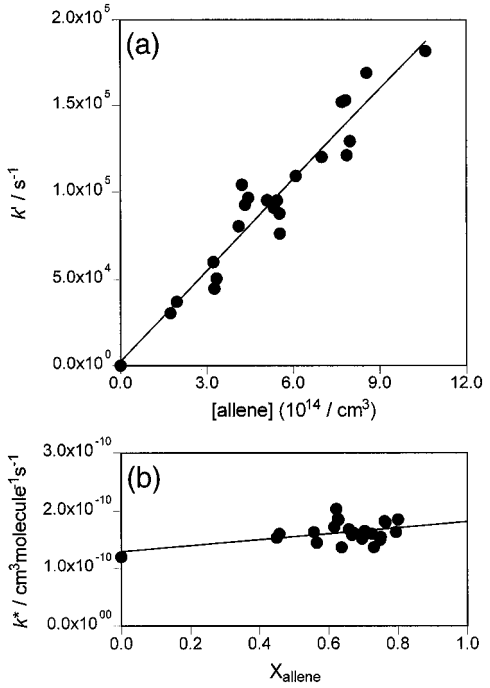

Figure 2. (a) Plot of k' vs $[CH_2CCH_2]$ yielding $k_{CH_2CCH_2} = (1.7 \pm 0.2) \times 10^{-10}$ cm^3 molecule^{-1} s^{-1}. (b) Plot of k^* vs $X_{CH_2CCH_2}$; $k_{CH_2CCH_2} = (1.8 \pm 0.2) \times 10^{-10}$ cm^3 molecule^{-1} s^{-1}; intercept $= k_{C_2H_2} = (1.7 \pm 0.2) \times 10^{-10}$ cm^3 molecule^{-1} s^{-1}; $k_{C_2H_2} = (1.2 \pm 0.2) \times 10^{-10}$ cm^3 molecule^{-1} s^{-1} (from ref 9).

the above expression, and a plot of k^* vs $X_{C_3H_4}$ provides $k_{C_2H_2}$ as the y intercept at $X_{C_3H_4} = 0$ and $k_{C_3H_4}$ at $X_{C_3H_4} = 1$.

As expected, both methods yield identical values for $k_{C_3H_4}$. The former method has the advantage of utilizing very accurate values for k_{C_2H} obtained in previous experiments (uncertainty 10−15%).[8,9] The latter method, while providing $k_{C_2H_2}$ as well as $k_{C_3H_4}$, requires that a large range of $X_{C_3H_4}$ be examined. This is difficult due to the fast reaction of the ethynyl radical with acetylene. Typical ranges for $X_{C_3H_4}$ are 0.45−0.80. Even with this range, the statistical uncertainty in $k_{C_2H_2}$ can be over twice that of the previous studies unless measurements are also made at $X_{C_3H_4} = 0$. The statistical uncertainty for $k_{C_3H_4}$ is independent of the method used. This latter method does provide a useful and convenient check of the experimental data. Plots of k' vs $[C_3H_4]$ and k^* vs $X_{C_3H_4}$ are shown in Figure 2 and the experimental results are given in Table 1.

TABLE 1: Summary of Rate Constants for $C_2H + C_3H_4$ (cm^3 molecule^{-1} s^{-1})

temp, K	k_{CH_3CCH}	temp, K	$k_{CH_2CCH_2}$
298	$(1.9 \pm 0.3) \times 10^{-10}$	297	$(1.7 \pm 0.3) \times 10^{-10}$
262	$(2.1 \pm 0.2) \times 10^{-10}$	242	$(2.1 \pm 0.3) \times 10^{-10}$
222	$(2.4 \pm 0.3) \times 10^{-10}$	215	$(2.7 \pm 0.6) \times 10^{-10}$
189[a]	$(2.4 \pm 0.4) \times 10^{-10}$	193	$(2.2 \pm 0.3) \times 10^{-10}$
179	$(2.1 \pm 0.3) \times 10^{-10}$	165	$(1.9 \pm 0.2) \times 10^{-10}$
157	$(1.9 \pm 0.2) \times 10^{-10}$	159[a]	$(2.4 \pm 0.3) \times 10^{-10}$
155[a]	$(2.4 \pm 0.3) \times 10^{-10}$		

[a] Measurements made under *high flow* conditions (see text).

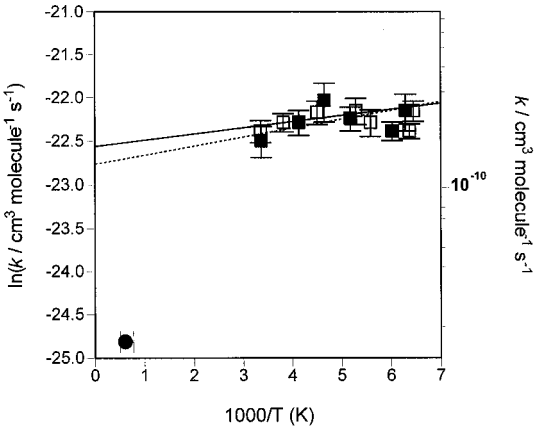

Figure 3. Arrhenius plot for $C_2H + C_3H_4$: (open squares) methylacetylene (propyne), (solid line) $k_{CH_3CCH} = (1.9 \pm 0.6) \exp[(22 \pm 80)]$ cm^3 molecule^{-1} s^{-1}; (solid squares) allene (propadiene), (dashed line) $k_{CH_2CCH_2} = (1.6 \pm 0.8) \exp[(55 \pm 68)]$ cm^3 molecule^{-1} s^{-1}. Filled circle, estimate for hydrogen abstraction reaction (from ref 15).

The uncertainties for $k_{C_3H_4}$ are determined by computing the standard deviation of the mean for each linear least-squares fit of the data. The standard deviation of each rate constant at a given temperature is taken as the overall experimental uncertainty (20−30%). For all results, the reported uncertainty is $\pm 2\sigma$. The data can be expressed using the Arrhenius form $k_{C_3H_4} = A \exp[(-E_a)/(RT)]$. The Arrhenius plot for both $C_2H + C_3H_4$ reactions over the experimental temperature range 155 K < T 298 K is shown in Figure 3. The rate coefficients are independent of pressure over the range 2.8−12 kPa (21−90 Torr) and laser fluence (15−50 mJ/pulse, 10 Hz) at room temperature.

Discussion

The reaction rates of C_2H with CH_3CCH and CH_2CCH_2 are very similar to those of other unsaturated hydrocarbons measured in our laboratory; the reactions are fast and show no temperature dependence or a slight negative temperature dependence.[8,10] The Arrhenius plot shown in Figure 3 displays the current results for the reactions 1 and 2. Both data sets show a slight negative temperature dependence down to 210−220 K, with a leveling off of the rate constants below 200 K. While an apparent change in slope may be interpreted as a varying temperature dependence caused by a competing mechanism, the most likely reason for this change is condensation of the reactant

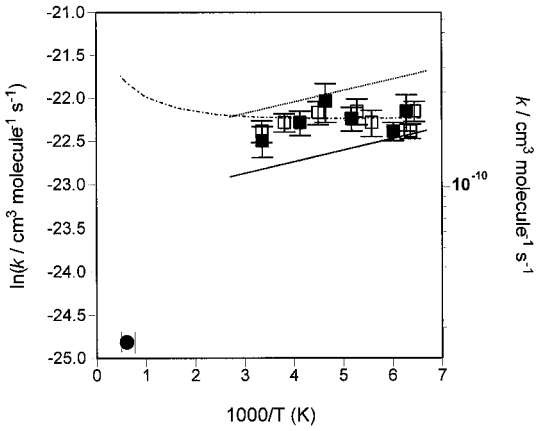

Figure 4. Arrhenius plot for $C_2H + C_3H_4$: (open squares) methylacetylene (propyne); (solid squares) allene (propadiene); (solid line) $k_{C_2H_4}$; (dashed line) $2k_{C_2H_4}$; (dash-dot curve) Lennard-Jones corrected rate constant for $C_2H + CH_2CCH_2$ scaled by the probability factor 0.27; (filled circle) estimate for hydrogen abstraction reaction (from ref 15).

on the walls of the flow tube. Several experiments were carried out below 200 K under *high flow* conditions where the buffer gas flow was increased from typical values of 300 sccm to approximately 700 sccm. The upper limit is set by the conductance of the flow cell and available pumping speed. These measurements produced rate constants ≈25% higher than those under normal flow conditions. Fitting all of the experimental data gives $k_{CH_3CCH} = (1.9 \pm 0.6) \exp[(22 \pm 80)/T]$ cm^3 molecule^{-1} s^{-1} and $k_{CH_2CCH_2} = (1.6 \pm 0.8) \exp[(55 \pm 68)/T]$ cm^3 molecule^{-1} s^{-1}. Excluding measurements below 180 K that were made under normal flow conditions gives the values $k_{CH_3CCH} = (1.6 \pm 0.4) \times 10^{-10} \exp[(71 \pm 50)/T]$ cm^3 molecule^{-1} s^{-1}, $k_{CH_2CCH_2} = (1.3 \pm 0.6) \times 10^{-10} \exp[(103 \pm 136)/T]$ cm^3 molecule^{-1} s^{-1}. The large uncertainties in E_a are the direct result of the difficulty in making measurements at the lowest temperatures. Efforts are currently underway to develop a new experimental technique that will improve and extend the low-temperature limits using a nozzle expansion.

The observed rate coefficients and slightly negative or zero temperature dependence are consistent with previous work with C_2H + unsaturated hydrocarbons.[8−10] These previous experiments showed the rate coefficients for reactions of C_2H with acetylene and ethene to be essentially equal. The lower solid line in Figure 4 is $k_{C_2H_4}$ from the Arrhenius fit to C_2H + ethene. Both k_{CH_3CCH} and $k_{CH_2CCH_2}$ are faster than $k_{C_2H_2}$ and $k_{C_2H_4}$. For CH_3CCH, the increase of the observed rate coefficient over $C_2H + C_2H_2$ is most likely due to the electron donating effect of the methyl group. Because this reaction is exothermic, −80 to −120 kJ mol^{-1}, the expected transition state is expected to occur early in the formation of the adduct, reducing steric effects of the methyl group. Although allene contains two double bonds, the reaction does not occur at twice the reaction rate as would be expected using the additivity rule ($k_{CH_2CCH_2} < 2k_{C_2H_4}$).[23] The upper dotted line in Figure 4 shows $2k_{C_2H_4}$.

While gas-kinetic collision rate coefficients give reasonable estimates for the reactions studied here, the Lennard-Jones corrected rate constant provides a more realistic model for radical−molecule reactions,[24] providing a correction due to attractive intermolecular forces.[25] The rate constant, Z_{12}, is given by

$$Z_{12} = \sigma_{12}^2 \Omega(2,2)^* (8\pi kT/\mu)^{1/2} \qquad (12)$$

where σ_{12} is the collision diameter, $\Omega(2,2)^*$ are tabulated collision integrals, k is Boltzmann's constant, T is the temperature, and μ is the reduced mass of the colliding molecules. The collision integrals are tabulated as functions of the reduced temperature T^*, which is a function of the absolute temperature and the Lennard-Jones force constant, $T^* = kT/\epsilon_{12}$.[26] Force constants and collisional diameters are determined using empirical combining rules ($\epsilon_{12} = (\epsilon_1\epsilon_2)^{1/2}$; $\sigma_{12} = (\sigma_1 + \sigma_2)/2$) and by assigning to C_2H the same Lennard-Jones parameters as C_2H_2. Comparison of the Z_{12} values with experimental rate coefficients indicates the reaction probability to be 0.40 for $C_2H + CH_3CCH$ and 0.27 for $C_2H + CH_2CCH_2$. A plot of the scaled values for Z_{C_2H,CH_2CCH_2} over the temperature range of 150−2000 K is shown as the dash-dot curve in Figure 4. The scaled values for Z_{C_2H,CH_3CCH} closely follow Z_{C_2H,CH_2CCH_2} and are omitted from Figure 4 to avoid congestion. The observed temperature dependence is in good agreement with the experimental results and the assumed addition−elimination mechanism. Measurements are needed at higher temperatures to determine if an increase in the reaction rate follows the Lennard-Jones corrected rate. It should be noted that the current work closely parallels results obtained for the room temperature rate constant of CN (which is isoelectronic with C_2H) with CH_3CCH and the temperature-dependent rate coefficients of CN with CH_2CCH_2.[23,27] While this study represents the first direct measurement for these rate coefficients, one previous study determined the ratio of the two addition−elimination reaction pathways shown in reaction 3 and below.[14]

$$C_2H + CH_3CCH \rightarrow C_4H_2 + CH_3 \qquad (13)$$

$$\rightarrow C_5H_4 + H \qquad (14)$$

The analysis by Cullis *et al.* determined k_{13}/k_{14} to be 10 ± 1 and the rate constant ratio for the reaction

$$C_2H + C_3H_4 \rightarrow C_2H_2 + C_3H_3 \qquad (15)$$

with reaction 14 determined to be 25 ± 3. This implies the rate constant for the hydrogen abstraction reaction would be over an order of magnitude faster than the addition/elimination pathway. In contrast, Wu and Kern have provided a much smaller estimate for the hydrogen abstraction reactions for reactions 3 and 4 of 1.67×10^{-11} cm^3 molecule^{-1} s^{-1}.[15] This value is shown in Figures 3 and 4 for reference. In the absence of direct experimental data, the estimate provided by Wu and Kern is reasonable for the hydrogen abstraction reaction. On the basis of previous work with CH_3CN, which is isoelectronic with methylacetylene, hydrogen abstraction from the methyl group is significantly slower than the proposed addition/elimination mechanisms.[12] Direct abstraction of the acetylenic hydrogen, a process that is thermoneutral, is also expected be relatively slow. However, recent kinetic data for saturated hydrocarbons with two or more carbons suggest that long-range attractive forces can play an important role for radical−molecule reactions, resulting in relatively fast rate coefficients and zero or slightly negative temperature dependencies.[11,28] Farrell and Taatjes have measured the HCl production for Cl atom reactions with both C_3H_4 isomers.[18] In their work, the reaction of Cl with allene at room temperature is suggestive of an addition and the formation of the resonance-stabilized chloroallyl radical.[18] For the reaction of Cl with methylacetylene between temperatures of 292−400 K, their results were consistent with competing abstraction and addition−elimination pathways. The fast rates and zero-to-slightly-negative temperature dependencies found in the present work are indicative of reactions being dominated

by addition−elimination processes. Further experimental work on the ethynyl + C_3H_4 systems is necessary to characterize the products and branching ratios for these chemical reactions.

Although methylacetyene and allene are both included in atmospheric models of Titan and Jupiter, the chemical/physical processes of these species have been limited to reactions with hydrogen atoms, photolysis, and condensation. Reactions of the ethynyl radical with methylacetylene and allene are not included in current photochemical models, yet reaction pathways for chemical species with similar concentrations are included. These chemical species include diacetylene, cyanoacetylene, and cyanogen. Each of these species as well as methylacetylene has been identified in the atmosphere of Titan.[29] As models become more complete, reaction pathways such as those studied here will also be included.

Acknowledgment. We gratefully acknowledge the National Aeronautics and Space Administration for support of this research.

References and Notes

(1) Lunine, J. I. *Mercury* **1997**, *10*, 10.
(2) Raulin, F.; Bruston, P.; Coll, P.; Coscia, D.; Gazeau, M.-C.; Guez, L.; DeVanssay, E. *J. Biol. Phys.* **1994**, *20*, 39.
(3) . Lara, L. M.; Lellouch, E.; Lopez-Moreno, J. J.; Rodrigo, R. *J. Geophys. Res.* **1996**, *101*, 261.
(4) Toublanc, D.; Parisot, J. P.; Brillet, J.; Gautier, D.; Raulin, F.; McKay, C. P. *Icarus* **1995**, *113*, 2.
(5) Yung, Y. L.; Allen, M.; Pinto, J. P. *Astrophys. J. Suppl.* **1984**, *55*, 465.
(6) Yung, Y. L. *Icarus* **1987**, *72*, 468.
(7) Gladstone, G. R.; Allen, M.; Yung, Y. L. *Icarus* **1996**, *119*, 1.
(8) Pedersen, J. O. P.; Opansky, B. J.; Leone, S. R. *J. Phys. Chem.* **1993**, *97*, 6822.
(9) Opansky, B. J.; Leone, S. R. *J. Phys. Chem.* **1996**, *100*, 4888.
(10) Opansky, B. J.; Leone, S. R. *J. Phys. Chem.* **1996**, *100*, 19904.
(11) Hoobler, R. J.; Leone, S. R. *J. Phys. Chem. A* **1997**, *101*, 1338.
(12) Hoobler, R. J.; Leone, S. R. *J. Geophys. Res.* **1997**, *102*, 28717.
(13) Opansky, B. J.; Seakins, P. W.; Pedersen, J. P. O.; Leone, S. R. *J. Phys. Chem.* **1993**, *97*, 8583.
(14) Cullis, C. F.; Hucknall, D. J.; Shepherd, J. V. *Proc. R. Soc. London A* **1973**, *335*, 525.
(15) Wu, C. H.; Kern, R. D. *J. Phys. Chem.* **1987**, *91*, 6291.
(16) Weast, R. C., Ed. *CRC Handbook of Chemistry and Physics*; CRC: Boca Raton, FL, 1990.
(17) Lowry, T. H.; Richardson, K. S. *Mechanisms and Theory in Organic Chemistry*; Harper and Row: New York, 1987.
(18) Farrell, J. T.; Taatjes, C. A. *J. Phys. Chem. A* **1998**, *102*, 4846.
(19) Song, X.; Bao, Y.; Urdahl, R. S.; Gosine, J. N.; Jackson, W. M. *Chem. Phys. Lett.* **1994**, *217*, 216.
(20) Satyapal, S.; Bersohn, R. *J. Phys. Chem.* **1991**, *95*, 8004.
(21) Yan, W.-B.; Dane, C. B.; Zeitz, D.; Hall, J. L.; Curl, R. F. *J. Mol. Spectrosc.* **1987**, *123*, 486.
(22) Hall, J. L.; Lee, S. A. *Appl. Phys. Lett.* **1976**, *29*, 367.
(23) Butterfield, M. T.; Yu, T.; Lin, M. C. *Chem. Phys.* **1993**, *169*, 129.
(24) Lee, J. H.; Michael, J. V.; Payne, W. A.; Stief, L. J. *J. Chem. Phys.* **1978**, *69*, 3069.
(25) Steinfled, J. I.; Francisco, J. S.; Hase, W. L. *Chemical Kinetics and Dynamics*, 1st ed.; Prentice Hall: Englewood Cliffs, NJ, 1989.
(26) Herschfelder, J. O.; Curtiss, C. F.; Bird, R. B. *Molecular Theory of Gases and Liquids* 1st ed.; John Wiley and Sons: New York, 1954.
(27) Sayah, N.; Li, X.; Caballero, J. F.; Jackson, W. *J. Photochem. Photobiol., A: Chem.* **1988**, *45*, 177.
(28) Sims, I. R.; Queffelec, J. L.; Travers, D.; Rowe, B. R.; Herbert, L. B.; Karthäuser, J.; Smith, I. W. M. *Chem. Phys. Lett.* **1993**, *211*, 461.
(29) Coustenis, A. *Ann. Geophys.* **1990**, *8*, 645.